Experimental investigations of micromachining characteristics on polydimethylsiloxane (PDMS) by cryogenic micro abrasive jet machining

Guiguan Zhang
Nanjing University of Aeronautics and Astronautics College of Mechanical and Electrical Engineering
https://orcid.org/0000-0003-2696-0205
Yuli Sun (sunyuli@nuaa.edu.cn)
Nanjing University of Aeronautics and Astronautics College of Mechanical and Electrical Engineering
Hang Gao
Dalian University of Technology
Dunwen Zuo
Nanjing University of Aeronautics and Astronautics College of Mechanical and Electrical Engineering

Original Article

Keywords: PDMS, CMAJM, Microchannel, Cryogenic, Erosion

Posted Date: December 28th, 2020

DOI: https://doi.org/10.21203/rs.3.rs-132645/v1

Abstract

In this study, a cryogenic micro-abrasive jet machining (CMAJM) experimental system is designed and built based on the glass transition characteristics of polydimethylsiloxane (PDMS). Fixed processing parameters are then used to evaluate the effectiveness of machining PDMS by micro-abrasive jet machining (MAJM) at room and cryogenic temperatures, and the results show that cryogenic could improves the processing quality of PDMS. Based on this, experiments are conducted into how microchannel processing quality is influenced by the scanning speed and the erosion distance, pressure, and angle. The results show that better PDMS microchannels are processed when the erosion distance is 2.5–3.5 μm, the erosion pressure is 0.4 MPa, the erosion angle is 60–75°, and the scanning speed is 0.25 mm/s.

1. Introduction

Micro-abrasive jet machining (MAJM) is a nontraditional machining technology that is distinct from traditional blasting processing[1–2]. It has been used to machine microstructural features such as holes and microchannels in hard and brittle materials such as silicon[3], glass[4], and acrylic[5]. Compared with processing methods such as deep reactive-ion etching[6] and laser ablation[7], MAJM has the advantages of high processing surface integrity, processing flexibility, and high material removal rate (MRR)[8]. Meanwhile, polymers such as polydimethylsiloxane (PDMS) are being used increasingly in microfluidics because of their excellent physical, chemical, and biological properties[9]. However, the typical elastomer characteristics of PDMS at room temperature mean that subjecting it to MAJM often leads to low MRR and serious abrasive embedding[10], among other problems. This makes it difficult to meet the high quality requirements of microfluidic chips, thereby limiting severely the use of MAJM in PDMS-based microfluidics.

As is well known, PDMS undergoes a glass transition at cryogenic temperatures (glass transition temperature Tg = 150 K), after which its mechanical properties differ significantly from those at normal temperatures[11]. In recent years, to improve the processing quality of difficult-to-machine materials, the technology of cryogenic high-efficiency precision machining has been developed[12–13]. Matthias et al.[14] found the elastic modulus of elastomer materials in the glass state to be increased substantially compared to those in the elastic state. While large processing deformations and poor surface quality arise during cutting at room temperature, precision processing based on brittle fracture can be realized at cryogenic temperature (glass state). Based on this, Song et al.[15] proposed cryogenically assisted micro-milling processing technology for PDMS based on compensationoferror mechanism; experimental results showed that as the temperature decreased, so did the roughness of the bottom surface of the processed microchannel. Spelt and colleagues[16–17] used external-mix and liquid nitrogen (LN_2) immersion experimental devices to study PDMS subjected to cryogenic micro-abrasive jet machining (CMAJM); the results showed that abrasive embedding was ameliorated significantly during the erosion of PDMS at cryogenic temperature and the erosion removal rate of PDMS was increased, thereby showing the feasibility of using CMAJM to machine PDMS materials.

In previous studies, Li et al.[18]; Valverde et al.[19] and Jafar et al.[20] carried out an experimental study on the roughness of surfaces machined by MAJM. They showed that the eroded surface morphology is related to parameters such as the erosion kinetic energy, abrasive mass flow rates and angle. Moreover, in microfluidics, microchannel surface roughness has an important influence on the flow characteristics[21]; for example, in microfluidics, the rougher the microchannel surface, the lower the separation efficiency[22–23] and electro-osmotic mobility[24]. Therefore, microchannel surface roughness is an important factor that cannot be ignored in MAJM.

In a microfluidic chip, microchannels in its substrate allow fluid to flow from one place to another to realize microfluidic transmission and mixing, which are the basic features of microfluidic chips. Sayah et al.[25] noted that the mixing performance of a micro-mixer was affected significantly by the microchannel cross-sectional shape. They used MAJM to machine three microchannels with different cross-sectional shapes on glass, and a microfluidic mixing experiment was conducted[26]; the results showed that changing the microchannel cross-sectional shape changed the microfluidic turbulence characteristics, thereby increasing the microfluidic mixing efficiency. Also, as microfluidic technology gradual development, microchannels with high aspect ratio and vertical sidewalls have become prevalent for microfluidic chips because of their long light transmittance, high channel density, and small bending effect[27].

Therefore, the present study explores the processing characteristics of PDMS at both room and cryogenic temperatures and then analyzes the advantages of PDMS machined by CMAJM by discussing these two different processing technologies (MAJM and CMAJM). Based on this, how the processing parameters of scanning speed and erosion distance, pressure, and angle affect the microchannel profile characteristics (i.e., microchannel depth and sidewall inclination) of PDMS is studied comprehensively.

2. Materials And Methods

PDMS prepolymer is a colorless, odorless, nonvolatile viscous liquid at room temperature and is cured by the catalytic reaction of a cross-linking agent. Here, the PDMS substrate was prepared from Sylgard 184 (Dow Corning, USA). The PDMS prepolymer and cross-linking agent were mixed at the suggested ratio of 10:1 and stirred for 30 min, then the mixture was placed in a vacuum drying oven for 1 h and poured into the mold. Finally, the mixture was left standing in air for 30 min and was then cured in a constant-temperature drying oven (DZF-6210; Shanghai Jinghong Experimental Equipment Co., Ltd., China) at 353 K for 2 h. Fig.1 shows a schematic diagram of preparation process for PDMS substrate.

The experimental CMAJM system comprised a machining unit, a jet generating unit, and an LN_2 flow-path unit, as shown in Figure 2(a). From its tank (DPL-175; Furuise, China), the LN_2 was sprayed onto the surface of the PDMS substrate through the LN_2 flow-path unit at a pressure of 0.2 MPa, whereupon the machining unit completed the machining of the PDMS. The jet-generating unit was a precision blasting machine (Model K, Series II; Airbrasive Jet Technologies, USA) that allowed the blasting pressure to be adjusted rapidly according to the experimental needs. The machining unit was controlled by a selfdeveloped closed-chamber four-dimensional mobile work table to achieve CMAJM. The device was equipped with a four-coordinate computer numerical control (CNC) system, and the processing parameters (e.g., scanning speed, erosion distance) could be adjusted automatically via NC codes. During the machining process, to minimize the influence of the LN_2 and abrasive jets on the abrasive erosion path during the interaction, the two central axes were arranged at 10° to each other.

Two common types of abrasive particle in MAJM are Al_2O_3 and SiC ones. Of the two, SiC abrasives are more brittle[28, 29]; therefore, to avoid the abrasive particles breaking upon impact at cryogenic temperature, Al_2O_3 abrasives particles with an average diameter of 25 μm were used (Density ρ = 3.99 g/cm^3, Modulus of elasticity E = 330 GPa, Fracture Toughness KIC = 4.5 MPa•m^{½}). Figures 2(b) and 2(c) shows the scanning electron microscope (SEM) image and particle size distribution of Al_2O_3 abrasives. Currently, the experimental research into CMAJM for PDMS is in the preliminary stage, and there are few references to guide the selection of the processing parameters. Therefore, to study how different processing parameters affect the structural characteristics of microchannels, the processing characteristics of PDMS are analyzed at both room and cryogenic temperatures. Single-factor experiments are used to study how the processing parameters of scanning speed and erosion distance, pressure, and angle influence the microchannel profile characteristics (i.e., microchannel depth and sidewall angle) of PDMS during CMAJM. The settings of the processing parameters are given in Table 1, the microchannel profile features of the PDMS substrate was measured by a three-dimensional optical profiler (WYKO NT9100; Veeco, USA).

Table 1 Design of experiment

Factor	Level-1	Level-2	Level-3	Level-4	Level-5
Scanning speed, mm/s	0.25	0.5	1	1.5	2
Erosion distance, mm	1.5	2.5	3.5	4.5	5.5
Erosion angle, °	30	45	60	75	90
Erosion pressure, MPa	0.2	0.3	0.4	0.5	0.6

3. Results And Discussion

To compare the processing effects at room and cryogenic temperatures, fixed processing parameters were selected for the PDMS machining, namely an erosion pressure of 0.4 MPa, an erosion angle of 90°, an erosion distance of 1.5 mm, and a scanning speed of 0.25 mm/s. After processing, the surface morphology and roughness were measured using an SEM (Quanta FEG 250; FEI, USA) and a three-dimensional optical profiler, respectively; the surface roughness was measured in an area of 300 μm × 230 μm.

The eroded surface morphology, microchannel profile and bottom surface roughness of PDMS at different temperatures are shown in Figure 3 and 4, respectively. At room temperature, the elastomer PDMS material suffers from serious abrasive embedding during MAJM. Also, because of the obvious “impact thermal effect”[30] of the plastic material during MAJM, the PDMS is covered with a processing deterioration layer on the eroded surface [Figure 3(a)], which seriously affects the subsequent experimental performance. After one machining pass at room temperature, the average erosion depth of the PDMS microchannel was 99.24 μm [Figure 3(a)], the Sa value of the bottom surface roughness was 3.439 μm (Figure 4), and the ratio of erosion depth to processing time was 11.2 μm/s; after one machining pass at cryogenic temperature, the corresponding values were 137.19 μm [Figure 3(b)], 2.33 μm (Figure 4), and 14 μm/s. The results show that the cryogenic cooling improved the PDMS MRR and surface quality significantly.

With cryogenic assistance, the PDMS eroded surface quality is greatly improved [Figure 3(b)], which is because the PDMS during CMAJM is at a temperature that is much lower than its glass transition temperature (Tg = 150 K). Therefore, the PDMS undergoes a glass transition and becomes brittle; the elastic modulus of the PDMS increases sharply[31], which in turn changes its erosion response behavior. For a ductile material, the material removal mechanism depends mainly on micro-cutting at small angles. For a brittle material, the material removal mechanism depends mainly on brittle fracture at large angles. Therefore, using CMAJM causes PDMS to transition from ductile to brittle erosion removal behavior, thereby realizing high-efficiency and low-damage micromachining of PDMS.

Furthermore, to analyze experimentally the CMAJM processing characteristics of PDMS, the experimental parameters in Table 1 were used in single-factor experiments to evaluate how the processing parameters affect the microchannel profile characteristics (i.e., microchannel depth and sidewall angle) of the PDMS substrate. Fig.5 shows how the erosion distance influenced the microchannel depth and sidewall angle. The experimental conditions were an erosion angle of 90°, an erosion pressure of 0.4 MPa, a scanning speed of 0.25 mm/s, and one machining pass. With increasing erosion distance, the microchannel depth increased initially and then decreased, while the sidewall angle decreased initially and then increased. The largest microchannel depth was that for an erosion distance of 3.5 μm, and the smallest sidewall angle was that for an erosion distance of 2.5 μm. Therefore, the best microchannel processing was achieved with an erosion distance of 2.5–3.5 μm.

Upon ejection from the nozzle, the abrasive particles accelerate initially and then decelerate as the spraying distance increases[32]. The abrasive particles moved fastest when the erosion distance was 3.5 μm; that is, they had the highest impact kinetic energy, and thus the processing efficiency was the highest. Therefore, the erosion depth of the PDMS substrate was relatively large at this time. Also, the greater the erosion distance, the greater the divergence of the abrasive jet; with small erosion distance, the abrasive particles gather in a smaller processing area. Meanwhile, the cryogenic cooling causes the response of the PDMS to the abrasive particles to transition from ductile to brittle removal; that is, the MRR is larger at large angles. Therefore, the MRR in the bottom region of the microchannel is large, while that in the sidewall region is small, thereby leading to different sidewall angles under different processing parameters. First, with increasing erosion distance, the speed of the abrasive particles increases and they collide frequently in the microchannel, which increases the MRR of the microchannel sidewalls, thereby reducing the sidewalls angle. Second, with further increase of the erosion distance, the degree of jet divergence increases, which causes the central area of the microchannel to be removed by erosion at large angles, while the sidewall area of the microchannel is removed by erosion at small angles, thereby increasing the sidewall angle of the microchannel.

Fig.6 shows how the erosion pressure influenced the microchannel depth and sidewall angle. The experimental conditions were the same as before, namely an erosion distance of 3.5 mm, an erosion angle of 90°, a scanning speed of 0.25 mm/s, and one machining pass. With increasing erosion pressure, the microchannel depth increased gradually, and the experimental phenomenon can be explained by the impact velocity of abrasive particles increase with increasing erosion pressure, which in turn leads to higher MRR. However, with increasing erosion pressure, the sidewall angle also changes to varying degrees; that is, the sidewall angle is largest at an erosion pressure of 0.5 MPa and is reduced accordingly when the erosion pressure reaches 0.6 MPa. The main reason for this may be that with increasing impact kinetic energy of the abrasive particles, their complex collision and erosion behavior during the machining leads to an irregular change in the sidewall angle of the microchannel. This is a compromise issue when selecting processing parameters when considering the microchannel erosion depth and sidewall angle. Fortunately, when the erosion pressure is higher than 0.4 MPa, the PDMS erosion depth increases less, while the microchannel sidewall angle is small at 0.4 MPa. Therefore, the best microchannel processing is achieved with an erosion pressure of 0.4 MPa.

Fig.7 shows how the erosion angle influenced the microchannel depth and sidewall angle. The experimental conditions were the same as before, namely an erosion distance of 3.5 mm, an erosion pressure of 0.4 MPa, a scanning speed of 0.25 mm/s, and one machining pass. With increasing erosion angle, the microchannel depth and sidewall angle tended to increase initially and then decrease. The microchannel depth was largest when the erosion angle was 60°, which can be explained simply by the fact that PDMS undergoes a glass transition (i.e., material embrittlement) at cryogenic temperatures. Therefore, the PDMS MRR at large angles is greater than that at small angles. Also, the sidewall angle was smallest when the erosion angle was 75°, the main reason being that the “erosion effect” of the abrasive jet on the surface differs with impact angle; that is, the number of Al_2O_3 particles involved in the effective erosion process is different, and while the complex erosion behavior caused by the collision and rebound of abrasive particles under different erosion angles. Fortunately, however, the microchannel depth and sidewall angle exhibit the same trend with varying erosion angle. Therefore, the best microchannel processing is achieved with an erosion angle of 60–75°.

Fig.8 shows how the scanning speed influenced the microchannel depth and sidewall angle. The experimental conditions were the same as before, namely an erosion distance of 3.5 mm, an erosion angle of 90°, an erosion pressure of 0.4 MPa, and one machining pass. With increasing scanning speed, the microchannel depth decreased almost linearly, while the sidewall angle tended to increase linearly. The main reason for this was insufficient cooling of the PDMS, namely failure to reach the embrittlement state as the scanning speed was increased, which in turn reduced the MRR of the PDMS, that is, the depth of the microchannel decreased. At the same time, increasing the scanning speed reduced the erosion time of the abrasive jet on the PDMS, reduced the microchannel erosion depth, and increased the sidewall angle. Comprehensive comparison showed that the best microchannel processing is achieved with a scanning speed of 0.25 mm/s.

In summary, with an erosion distance of 2.5–3.5 μm, an erosion pressure of 0.4 MPa, an erosion angle of 60–75°, and a scanning speed of 0.25 mm/s, CMAJM produces the best microchannel processing.

4. Conclusions

Based on the glass transition characteristics of PDMS, CMAJM was used to micro-machining PDMS. The experiment focused on how the processing parameters influence the microchannel profile characteristics of PDMS (i.e., microchannel depth and sidewall inclination), and a reasonable analysis was put forward. The main conclusions of this study are as follows.

(1) CMAJM can realize the erosion processing of the elastomer PDMS material at a vertical angle. Compared with the processing results at room temperature, the microchannel depth by CMAJM increased by 38.2%. Also, the eroded surface had no obvious abrasive embedding or processing deformation layer, and the surface roughness was lower. The microchannel processing effectiveness is related to factors such as the scanning speed and the erosion distance, pressure, and angle, and it can improved by selecting reasonable processing parameters.

(2) This study has improved the processing quality of PDMS by experimental analysis and offers the possibility for the rapid preparation of direct-write microchannels on PDMS substrates. Also, the cryogenic temperature reduces the scattering of abrasive particles during processing and makes the processing technology more environmentally friendly.

5. Declarations

Acknowledgements

The authors sincerely thanks to Professor Wen-Zhuang Lu of Nanjing University of Aeronautics and Astronautics for his critical discussion and reading during manuscript preparation.

Funding

National Natural Science Foundation of China (Grant No.52075254), Postgraduate Research & Practice Innovation Program of Jiangsu Province (KYCX20_0183) and the Key Laboratory for Precision & Non-traditional Machining of Ministry of Education, Dalian University of Technology (JMTZ201901).

Availability of data and materials

The datasets supporting the conclusions of this article are included within the article.

Authors' contributions

The author' contributions are as follows: Yu-Li Sun was in charge of the whole trial; Gui-Guan Zhang wrote the manuscript; Hang Gao assisted with sampling; and Dun-Wen Zuo assisted with laboratory analyses.

Competing interests

The authors declare no competing financial interests.

Consent for publication

Not applicable

Ethics approval and consent to participate

Not applicable

References

1. R Melentiev, F Z Fang. Recent advances and challenges of abrasive jet machining. *CIRP Journal of Manufacturing Science & Technology*, 2019, 22: 1-20.
2. J C Aurich, B Kirsch, D Setti, D Axinte, H. Yamaguchi. Abrasive processes for micro parts and structures. *CIRP Annals-Manufacturing Technology*, 2019, 68(2): 653-676.
3. L P Shi, Y Fang, Q W Dai, W Huang, X L Wang. (2018). Surface texturing on SiC by multiphase jet machining with microdiamond abrasives. *Materials and Manufacturing Processes*, 2018, 33(13): 1415-1421.
4. J Hwang, Y H Cho, M S Park, B H Kim. Microchannel Fabrication on Glass Materials for Microfluidic Devices. *International Journal of Precision Engineering and Manufacturing*, 2019, 20(3): 479-495.

5. A Nouhi, J K Spelt, M Papini. Abrasive jet turning of glass and PMMA rods and the micro-machining of helical channels. *Precision Engineering*, 2018, 53: 151-162.
6. J Arab, P Dixit, P K Brahmankar, R S Pawade, A K Srivastava. Micro-Faraday cup array structures fabrication in silicon using deep reactive ion etching. *International Journal of Precision Technology*, 2020, 9(1): 37.
7. S Prakash, S Kumar. Fabrication of microchannels on transparent PMMA using CO2 Laser (10.6 μm) for microfluidic applications: An experimental investigation. *International Journal of Precision Engineering and Manufacturing*, 2015, 16: 361-366.
8. S S Hsieh, J K Kuo, C F Hwang, H H Tsai. A novel design and microfabrication for a micro PEMFC. *Microsystem Technologies*, 2004, 10(2): 121-126.
9. S Padilla, E Tufekcioglu, R Guldiken. Simulation and verification of polydimethylsiloxane (PDMS) channels on acoustic microfluidic devices. *Microsystem Technologies*, 2018, 24: 3503-3512.
10. H Getu, J K Spelt, M Papini. Cryogenically assisted abrasive jet micromachining of polymers. *Journal of Micromechanics and Microengineering*, 2008, 18(11): 115010(8pp).
11. D Axinte, Y B Guo, Z R Liao, J S Albert, R M Saoubie, N Sugitaf. Machining of biocompatible materials-Recent advances. *CIRP Annals-Manufacturing Technology*, 2019, 68(2): 629-652.
12. A Thakur, A Manna, S Samir. Performance Evaluation of Different Environmental Conditions on Output Characteristics During Turning of EN-24 Steel. *International Journal of Precision Engineering and Manufacturing*, 2019, 20(10): 1839-1849.
13. Y Natarajan, P K Murugasen, L R Sundarajan, R Arunachalam. Experimental Investigation on Cryogenic Assisted Abrasive Water Jet Machining of Aluminium Alloy. *International Journal of Precision Engineering and Manufacturing-Green Technology*, 2019, 6(3): 415-432.
14. P Matthias, D Martin, N Mike, S Torsten. Mechanism of Cutting Elastomers with Cryogenic Cooling. *CIRP Annals-Manufacturing Technology*, 2016, 65(1), 73-76.
15. K Song, G M Gang, M B G Jun, B K Min. Cryogenic machining of PDMS fluidic channel using shrinkage compensation and surface roughness control. *International Journal of Precision Engineering and Manufacturing*, 2017, 18(12), 1711-1717.
16. A G Gradeen, J K Spelt, M Papini. Cryogenic abrasive jet machining of polydimethylsiloxane at different temperatures. *Wear*, 2012, 274-275: 335-344.
17. A G Gradeen, M Papini, J K Spelt. The effect of temperature on the cryogenic abrasive jet micro-machining of polytetrafluoroethylene, high carbon steel and polydimethylsiloxane. *Wear*, 2014, 317(1-2): 170-178.
18. H Z Li, J Wang, N Kwok, T Nguyen, G H Yeoh. A study of the micro-hole geometry evolution on glass by abrasive air-jet micromachining. *Materials and Manufacturing Processes*, 2018, 31: 156-161.
19. G B Valverde, R Jimbo, H S Teixeira, E A Bonfante, M N Janal, P G Coelho. Evaluation of surface roughness as a function of multiple blasting processing variables. *Clinical Oral Implants Research*, 2013, 24: 238-242.

20. R H M Jafar, J. K Spelt, M Papini. Surface roughness and erosion rate of abrasive jet micro-machined channels: Experiments and analytical model. *Wear*, 2013, 303(1-2): 138-145.
21. J Jia, Q Song, Z Liu, B Wang. Effect of wall roughness on performance of microchannel applied in microfluidic device. *Microsystem Technologies*, 2019, 25(6): 2385-2397.
22. A Ghobeity, H J Crabtree, M Papini, J K Spelt. Characterisation and comparison of microfluidic chips formed using abrasive jet micromachining and wet etching. *Journal of Micromechanics and Microengineering*, 2012, 22(2): 025014-025023.
23. D S Park, M W Cho, H Lee, W S Cho. Micro-grooving of glass using micro-abrasive jet machining. *Journal of Materials Processing Technology*, 2004, 146(2): 234-240.
24. S Schlautmann, H Wensink, R Schasfoort, M Elwenspoek, A Berg. Powder-blasting technology as an alternative tool for microfabrication of capillary electrophoresis chips with integrated conductivity sensor. *Journal of Micromechanics and Microengineering*, 2001, 11(4): 386-389.
25. A Sayah, P A Thivolle, V K Parashar, M A M Gijs. Fabrication of microfluidic mixers with varying topography in glass using the powder-blasting process. *Journal of Micromechanics and Microengineering*, 2009, 19 (8): 85024.
26. D Solignac, A Sayah, S Constantin, R Freitag, M A M Gijs. Powder blasting for the realization of microchips for bio-analytic applications. *Sensors & Actuators A Physical*, 2001, 92(1-3): 388-393.
27. M L Hupert, J M Jackson, H Wang, M A Witek, J Kamande, M I Milowsky, Y E Whang, S A Soper. Arrays of high-aspect ratio microchannels for high-throughput isolation of circulating tumor cells (CTCs). *Microsystem Technologies*, 2014, 20(10-11): 1815-1825.
28. D Senthilkumar. Thermophysical behavior of cryogenically treated silicon carbide for nanofluids. *Materials and Manufacturing Processes*, 2014, 29(7): 819-825.
29. J N Brecker. The fracture strength of abrasive grains. *Journal of Engineering for Industry*, 1974, 96(4): 1253-1257.
30. R Melentiev, F Fang. Investigation of erosion temperature in micro-blasting. *Wear*, 2019, 420(1): 123-132.
31. G G Zhang, Y L Sun B K Qian, H Gao, D W Zuo. Experimental study on mechanical performance of polydimethylsiloxane (PDMS) at various temperatures. *Polymer Testing*, 2020, 90: 106670.
32. R Melentiev, F Fang. Theoretical study on particle velocity in micro-abrasive jet machining. *Powder Technology*, 2019, 344: 121-132.

Figures

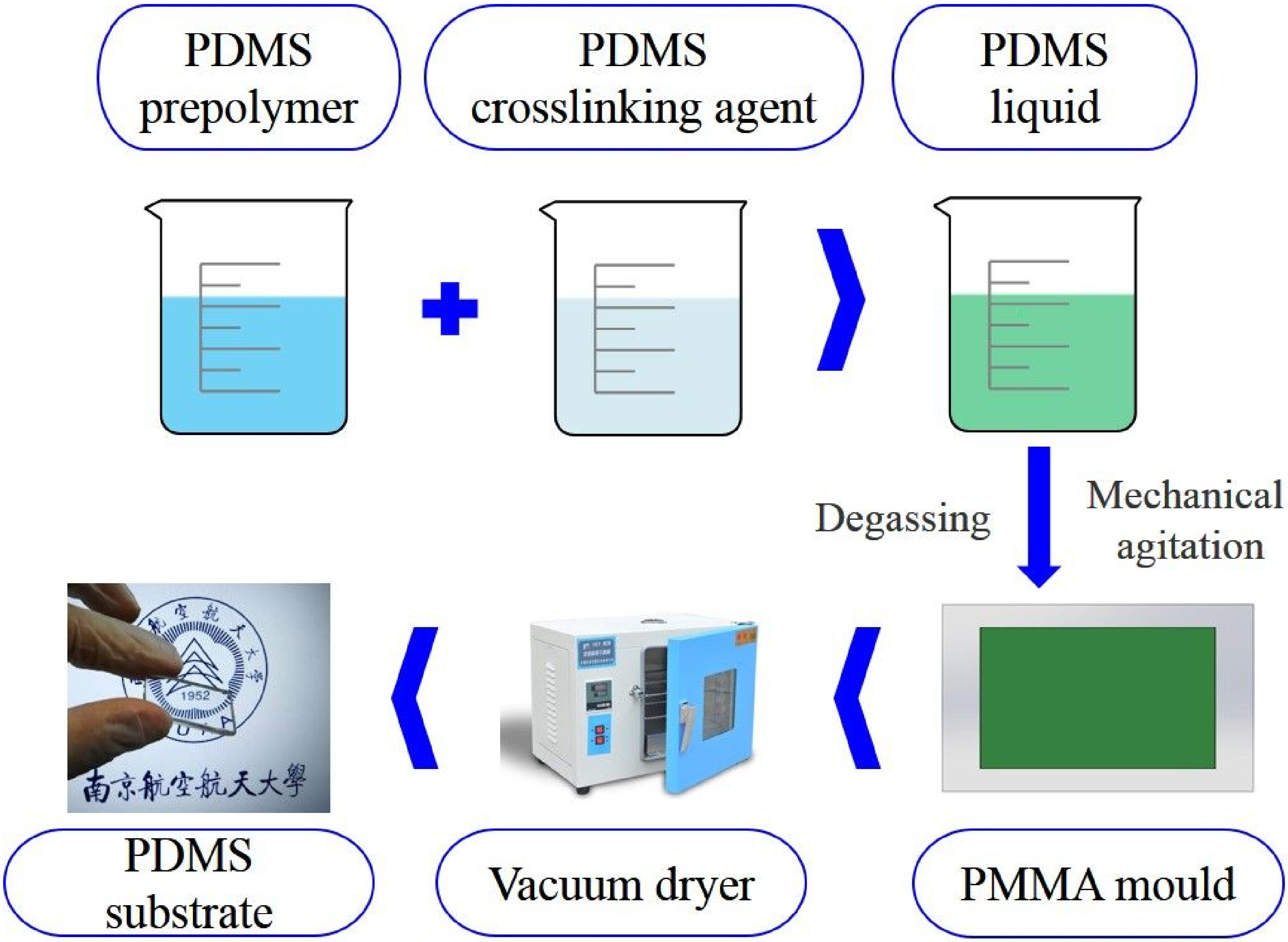

Figure 1

Schematic diagram of preparation process for PDMS substrate

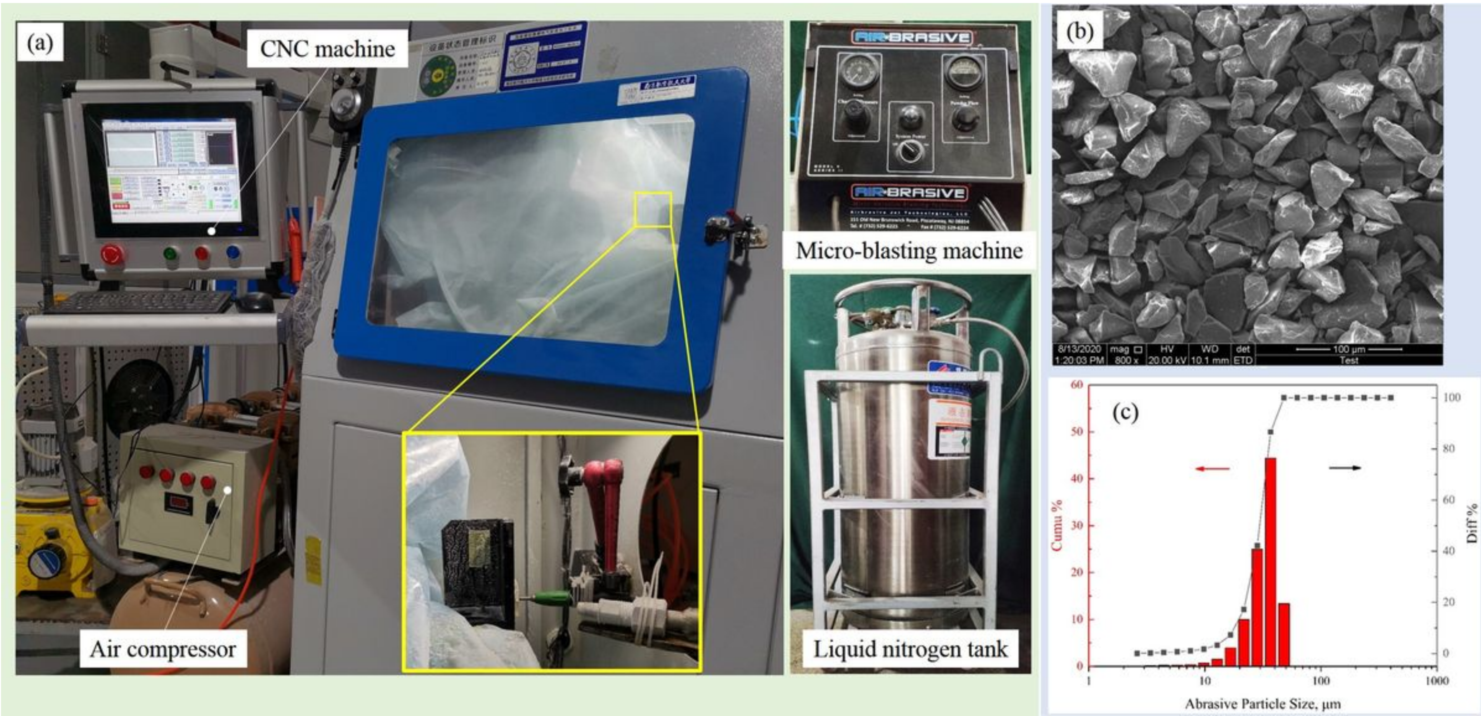

Figure 2

Experimental details: (a) experiment system of cryogenic micro-abrasive jet machining, (b) An SEM image and (b) size distribution of the Al2O3 particles (25 μm)

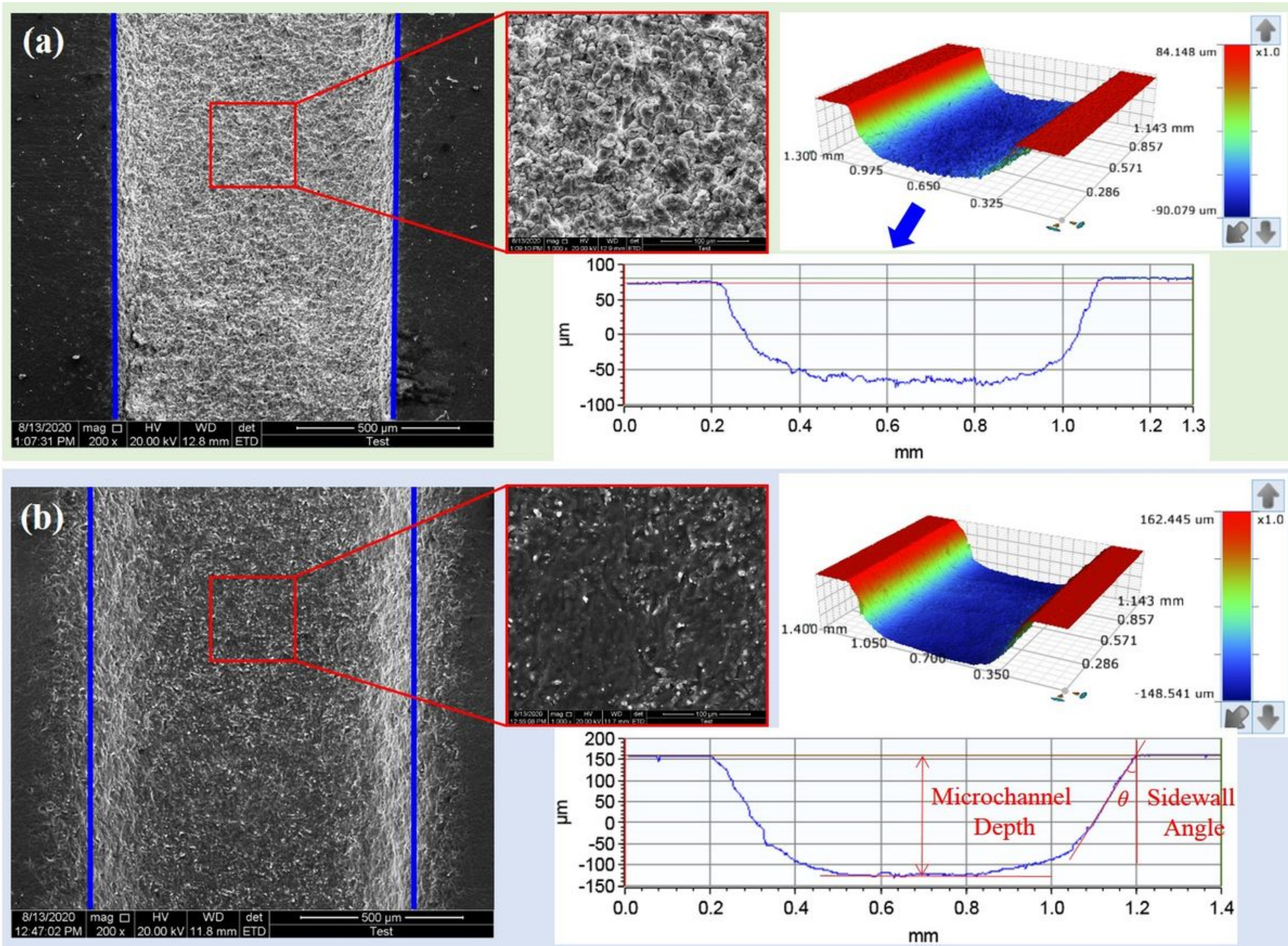

Figure 3

Typical processing results by different temperature: (a) room temperature and (b) cryogenic temperature

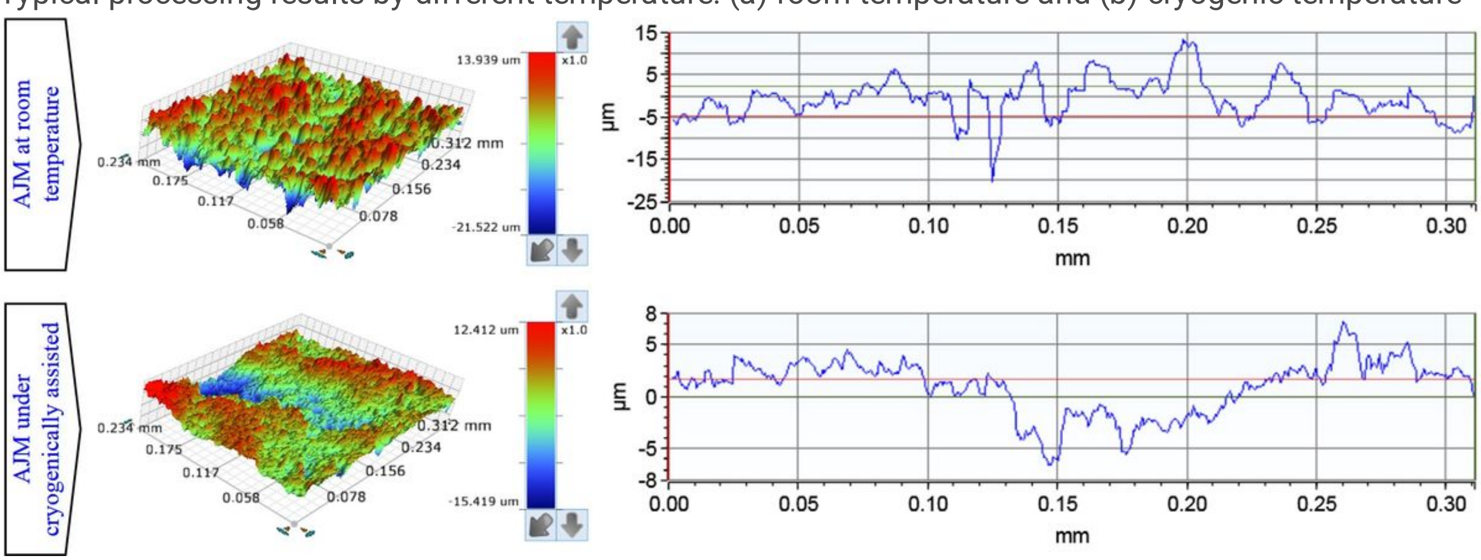

Figure 4

3D topography and 2D profile of the erosion surfaces. The initial (lapped) surface is on top. Note that the scale of the z-axis is different for each plot

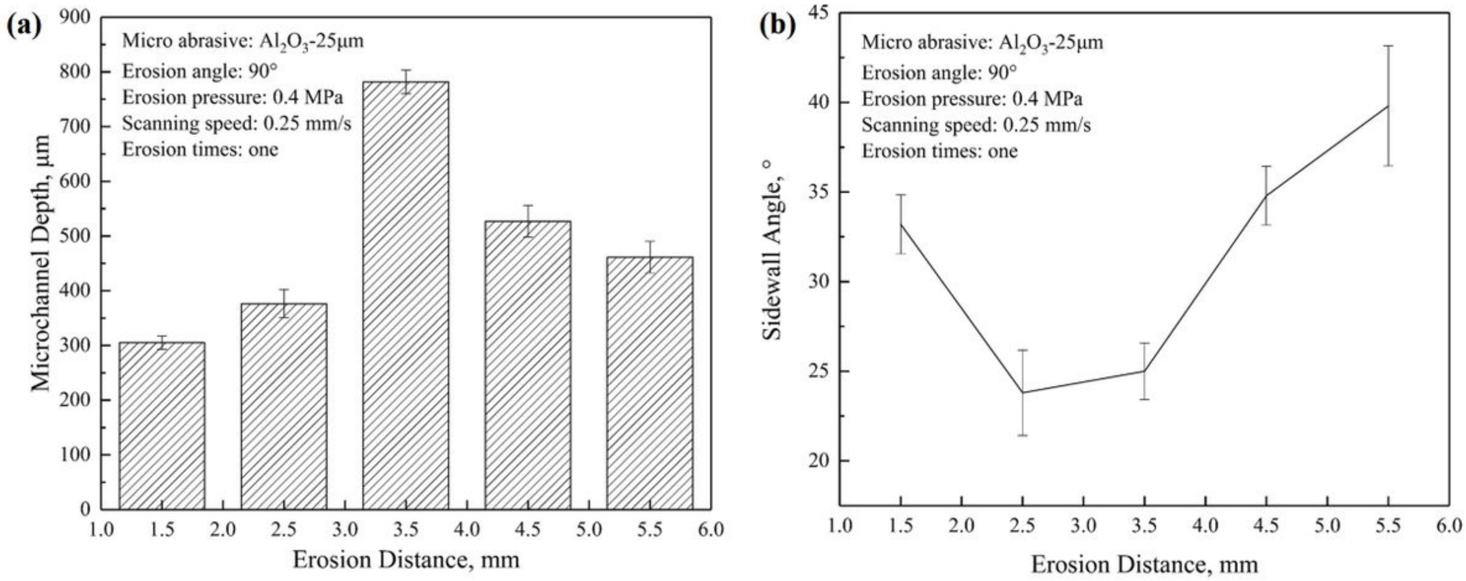

Figure 5

The effect of the erosion distance of nozzle on (a) erosion depth and (b) sidewall angle.

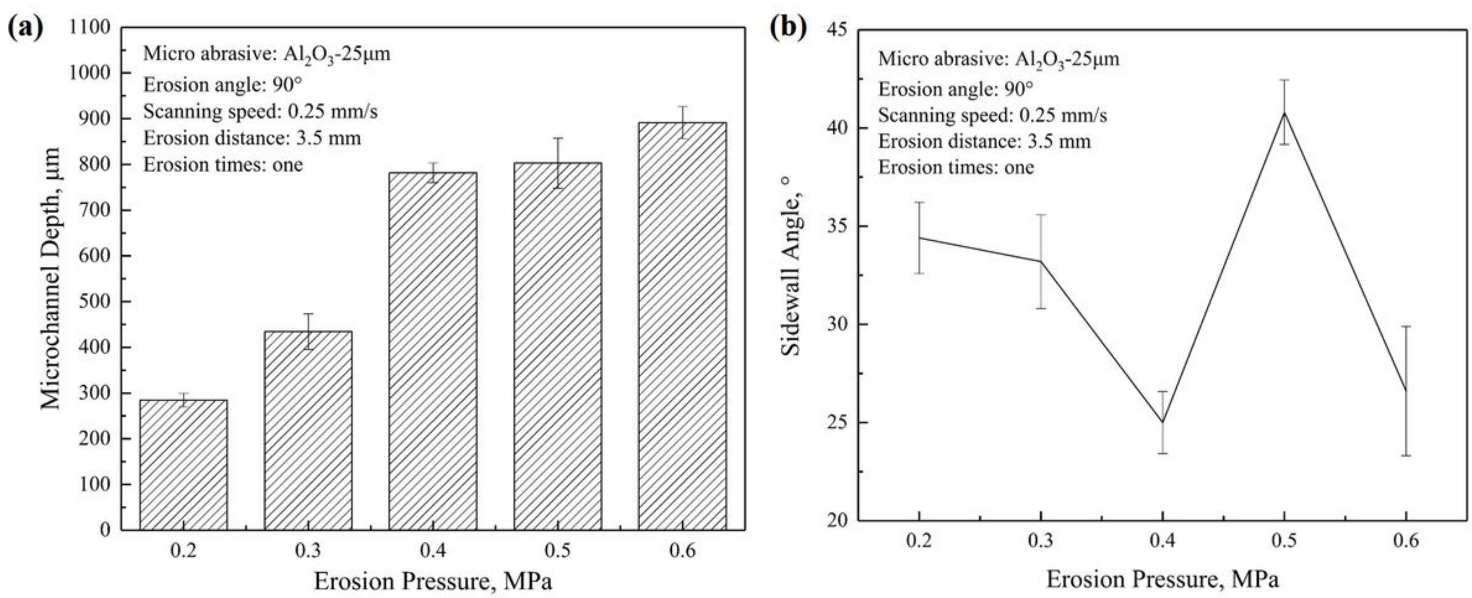

Figure 6

The effect of the impact pressure on (a) erosion depth and (b) sidewall angle.

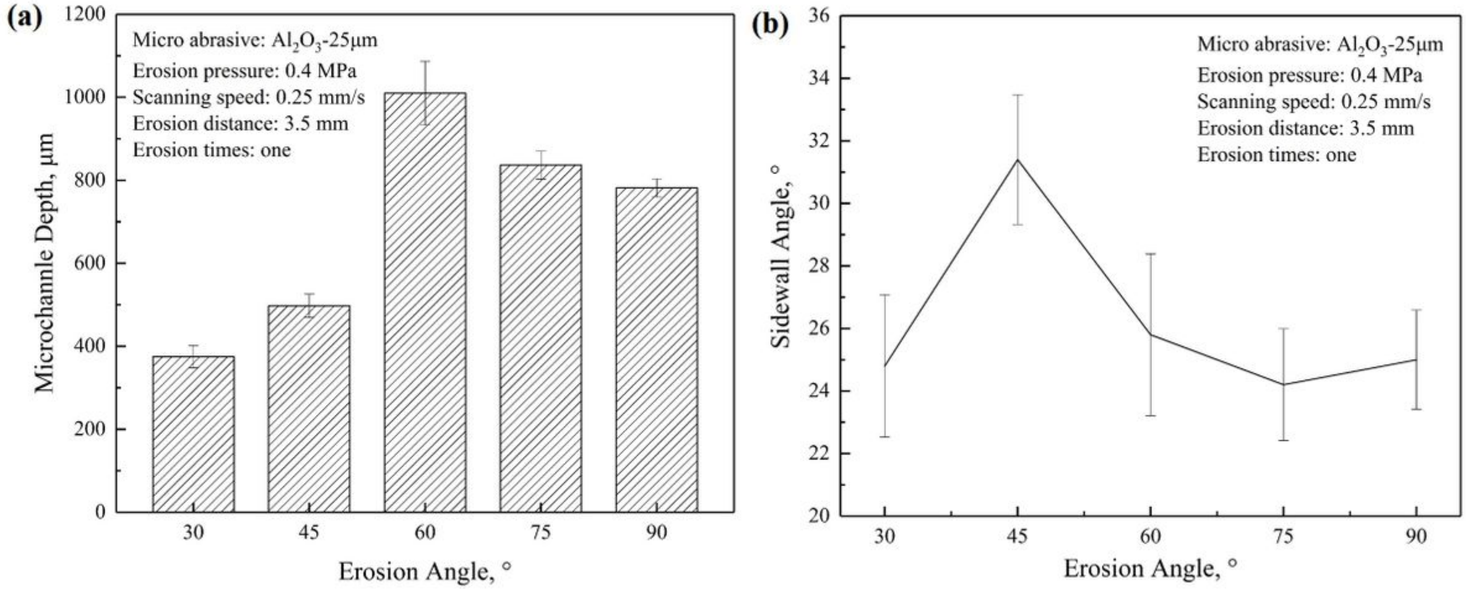

Figure 7

The effect of the impact angle on (a) erosion depth and (b) sidewall angle.

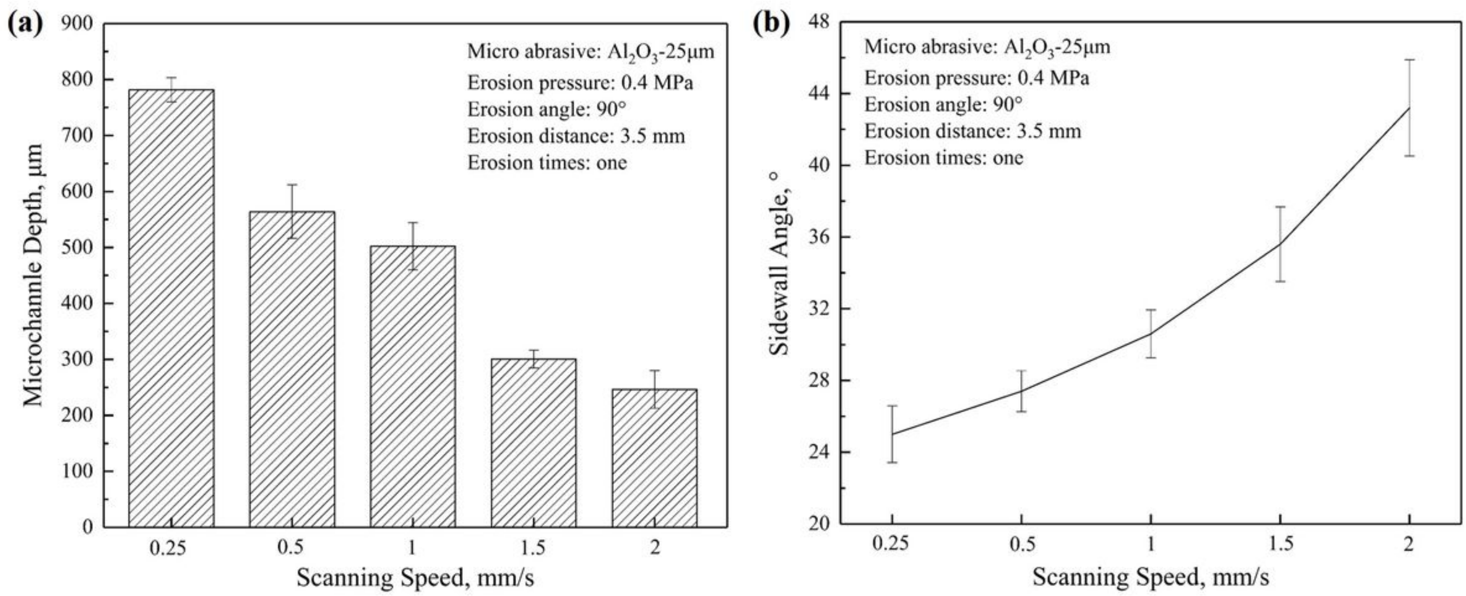

Figure 8

The effect of the scanning speed of nozzle on (a) erosion depth and (b) sidewall angle.